The Fast Wavelet Transform and its Application to Electroencephalography:

A Study of Schizophrenia

Prepared by:

Cullen Jon Navarre Roth

April 29, 2014

ACKNOWLEDGMENTS

I would like to thank the National Science Foundation for its support through the Fall of academic year of 2014 “Mentoring through Critical Transition Points” (MCTP) grant DMS 1148001. I would also like to thanks the Undergraduate Committee, especially Professor Monika Nitsche in her dual role as Chair of the Undergraduate Committee and PI of the MCPT grant. I would also like to thank Professors Christina Pereyra, Dr. David Bridwell, Dr. Navin Cota Gupta, Dr. Vince Calhoun, and Dr. Maggie Werner Washburne for their support and encouragement.

Table of Contents

Chapter 1 Introduction

Unveiling the transient world is a complex and compelling problem in applied mathematics. Numerous technologies and analytics have been created to study dynamic signals. The wavelet transform (WT) is one such tool. The WT grants us the ability to deconstruct multifaceted signals into time frequency representations which allows the user to zoom into and take apart an observed signal.

This ability of the wavelet transform is generated by multiresolution properties. Not only do these unique properties produce time series information regarding a signal but they also grant frequency information. With each level of deconstruction of a signal, we may observe different contributing waveforms to the signal in certain frequency bandwidths or intervals.

While the WT is unique, its applications are many. An area of application and the focus of this study is signal processing. Specifically the processing and analysis of electrical potentials generated from the scalp or more commonly named Electroencephalographic (EEG) responses.

These signals are of interest because they are a determinant of brain health and cognition. Individuals diagnosed with schizophrenia demonstrate a reduced event related potential (ERP) ~300 ms after a rare stimulus [24]. This response is associated with the reorganization toward unexpected events.

This study will explore the time-frequency characteristics of these responses and examine the degree in which responses are modulated by regularities in the environment within healthy individuals and individuals with schizophrenia.

Chapter 2 Preliminaries

2.1. The Wavelet Basis

A function $\psi \in L^2(R)$ is a wavelet if $\{\psi_{j,k} := 2^{\frac{j}{2}}\psi_{j,k}(2^j t - k) \text{ for } j, k \in Z\}$ forms an orthonormal basis for $L^2(R)$. This basis is called a wavelet basis. The wavelet transform involves the use of translations and scaling instead of modulations. This provides the wavelet transform with a natural zooming mechanic. We will talk more about this zooming mechanism in the Orthogonal Multiresolution section. With a wavelet transform the idea is to deconstruct a signal into an approximation and a set of details.

Definition The orthogonal wavelet transform is defined as the function that maps $L^2(R)$ the set of $L^2(R)$ itegrable functions to the *little l^2 of the Integers, over the complex numbers.* and assigns each function in $L^2(R)$ a sequence of wavelet coefficients:

$$W_j f(j,k) := \langle f, \psi_{j,k} \rangle = \int_R f(x)\overline{\psi_{j,k}(x)}\, dx \qquad (1)$$

2.2. Orthogonal Multiresolution Analysis (MRA):

Definition 10. [13,7] A multiresolution analysis (MRA) is a decomposition of $L^2(R)$the set of square integrable functions on R into a set of nested subspaces where V_0 is the central space. An MRA satisfies the following properties:

$$\forall\, j \in Z, \qquad V_{j+1} \subset V_j \qquad (2)$$

$$\forall\, j \in Z\,, f(t) \in V_j \Leftrightarrow f\left(\frac{t}{2}\right) \in V_{j+1} \qquad (3)$$

$$\lim_{j \to +\infty} V_j = \bigcap_{j=-\infty}^{+\infty} V_j = \{0\} \tag{4}$$

$$\lim_{j \to -\infty} V_j = closure\left(\bigcup_{j=-\infty}^{j=+\infty} V_j\right) = L^2(R) \tag{5}$$

The integer translates of the scaling function φ form an orthonormal basis for V_0 (6)

Definition 11. [Meyer] The scaling function mentioned in (6) we will define:

$$\varphi_{j,k}(t) \coloneqq 2^{\frac{-j}{2}} \varphi(2^{-j} t - k) \tag{7}$$

Assume the following theorem

Theorem 12. ([13], Theorem 7.1) Let $\{V_j\}_{j \in Z}$be an MRA with a scaling function φ whose dilations and translations according to (3.1.5) form an orthonormal basis of *V_0*. Then the family $\{\varphi_{j,k}\}_{k \in Z}$is also an orthonormal basis of $\{V_j\}_{j \in Z}$.

Briefly we will discuss the MRA and its properties. Property (2) states that the subspaces are nested. Each space expresses a level of detail that is contained in the subspace above.

$$\ldots V_3 \subset V_2 \subset V_1 \subset V_0 \subset V_{-1} \subset V_{-2} \subset V_{-3} \ldots$$

Here it is important to note that depending on the author the index of the subspaces may be different; for example, Matlab© software, [13],[7] has an increasing index with declining subspaces. In other words:

$$\lim_{j \to -\infty} V_j = L^2(R).$$

The scaling function allows us to climb upward and downward from space to space. This is seen in the scaling property (3).This property along with (6) allows us to calculate any detail in space at a resolution 2^{j+1} using only the information from the space above at a resolution 2^j. As the resolution gets worse $(j \to \infty)$ (3.1.4) implies that we will eventually lose all detail. Thus we can see that the scaling function, φ completely defines its MRA.

There is also a sequence of related orthogonal subspaces W_j of $L^2(R)$ that are related to our V_j. While not completely necessary, in an *orthogonal* MRA we require that $V_j \perp W_j$ for all j([7], [14]). These spaces are then connected in an MRA by

$$V_j = V_{j+1} \oplus W_{j+1}$$

Here we are using the "Matlab" indexing, where the space$V_{j+1} \subset V_j$. The $\oplus$symbol is the summation of the orthogonal spaces W_j of$L^2(R)$. When decomposing a signal, we start with the finest or "best" approximation for the signal and choose the lowest level of detail for decomposition. So we will have spaces nested:

$$V_n \subset \cdots V_3 \subset V_2 \subset V_1 \subset V_0$$

such that we can use the $\oplus$ symbol and truncate the information to attain:

$$V_0 = V_j \oplus_{j=1}^{n} W_j$$

Example 13. For the central space $V_0$when decomposed to 3 levels, we may represent the central space as

$$V_0 = V_1 \oplus W_1$$

$$V_0 = V_2 \oplus W_2 \oplus W_1$$

$$V_0 = V_3 \oplus W_3 \oplus W_2 \oplus W_1$$

In neurology the convention is to denote the spaces $\{W_3, W_2, W_1\}$ as *octaves* and the space V_3 as the *residual* space ([1],[2],[3],[4],[5]).

□

Theorem 14. [17](Mallat's Theorem).Given an orthogonal MRA with scaling function φ, there is a wavelet $\psi \in L^2(R)$ such that for each $j \in Z$, the family $\{\psi_{j,k}\}_{k\in Z}$ is an orthonormal basis for W_j. Hence the family $\{\psi_{j,k}\}_{k\in Z}$ is an orthonormal basis for $L^2(R)$.

From Mallat's Theorem, a central and basic tenant in multiresolution analysis, [7] whenever we have an MRA that satisfies (2) – (6) we have wavelet function defined as (from [Meyer])

$$\psi_{j,k} := 2^{\frac{-j}{2}} \psi_{j,k}(2^{-j}t - k) \tag{8}$$

Theorem 14 states that (8) exists, is determined by the scaling function φ, and forms an orthonormal wavelet basis for W_j. The W_j spaces in an orthogonal MRA are referred to as the wavelet spaces or *detail* spaces. A proof of Theorem 14 may be found in [17], [14], [13], and [7].

Returning to the definition of an MRA, it follows that the fifth property (5) of an *orthogonal* MRA may be restated as:

$$L^2(R) = \overline{\bigoplus_{j \in Z} W_j} \tag{9}$$

Where we have:

$$W_j = \overline{\operatorname{span}\{\psi_{j,k}\}}_{k\in Z} \tag{10}$$

Definition 15. For a signal (or function) $f(t)$ we will define the orthogonal projection of our signal onto the space V_j as

$$P_j f(t) = \sum_{k \in Z} \langle f, \varphi_{j,k} \rangle \varphi_{j,k}(t) \tag{11}$$

where $\langle f, \varphi_{j,k} \rangle$ is the inner product of our signal and scaling function (for a definition of the inner product please refer to the appendix).

Since $P_j f(t)$ is the orthogonal projection of our signal, it is the "best" approximation of our signal in V_j (see figure 1). From [13], as a consequence of (4)

$$\lim_{j \to +\infty} \|P_j f\|_2 = 0$$

Then for $P_{j+1} f(t) \in V_{j+1} \subset V_j$ the orthogonal projection $P_j f(t)$ will be a better approximation for our $f(t)$ than $P_{j+1} f(t)$ since V_{j+1} is nested in V_j.

The difference between our two approximations, $P_j f(t)$ and $P_{j+1} f(t)$ is the orthogonal projection of our signal $f(t)$ onto the orthogonal wavelet space W_{j+1} and can then be calculated

$$Q_{j+1} f(t) = P_j f(t) - P_{j+1} f(t) = \sum_{k \in Z} \langle f, \psi_{j+1,k} \rangle \psi_{j+1,k}(t) \tag{12}$$

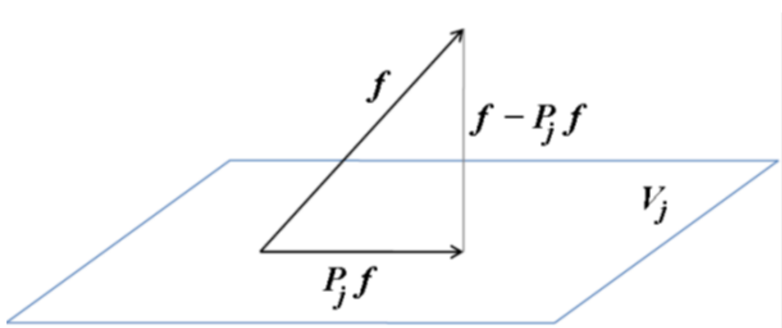

Figure 1. $\boldsymbol{P_j f}$ is the projection of f in the space V_j

Rewriting equation (12) and inserting equation (11) we obtain:

$$P_j f(t) = P_{j+1} f(t) + Q_{j+1} f(t)$$

$$P_j f(t) = \sum_{k \in Z} \langle f, \varphi_{j+1,k} \rangle \varphi_{j+1,k}(t) + \sum_{k \in Z} \langle f, \psi_{j+1,k} \rangle \psi_{j+1,k}(t) \qquad (13)$$

Chapter 3 Scaling Equation and Conjugate Mirror Conditions

"The multiresolution theory of orthogonal wavelets proves that any conjugate mirror filter characterizes a wavelet ψ that generates an orthonormal basis of $\mathbf{L}^2(R)$*."*

S. Mallat

In this chapter, we will discuss the connection between an MRA and scaling equations. This will then lead us to defining conjugate mirror filters.

3.1. The Scaling Equation

Remark 16 Recall (2) from our MRA because $\varphi \in V_0 \subset V_{-1}$ we may express φ as a superposition of $\varphi_{-1,k}$ where $\varphi_{-1,k}(t)$ forms an orthonormal basis of V_{-1}

$$\varphi_{-1,k}(t) = \sqrt{2}\varphi(2t-k), k \in Z \tag{14}$$

Meaning, there exists a sequence of coefficients $\{h_k\}_{k\in Z}$ that satisfy the following scaling equation.

$$\varphi(t) = \sum_{k\in Z} h_k \varphi_{-1,k}(t) = \sqrt{2}\sum_{k\in Z} h_k\, \varphi(2t-k) \tag{15}$$

The sequence of coefficients $\{h_k\}_{k\in Z}$ are given by the inner product

$$h_k := \langle \varphi, \varphi_{-1,k} \rangle \tag{16}$$

These coefficients $\{h_k\}_{k\in Z}$ are the so called *low pass filter*. They are often produced from a trigonometric polynomial (such as a *spline* function discussed later) with a period of one and with only a few of the coefficients not equal to zero. Thus they are referred to as *finite impulse response filters* (FIR) [13], [7]. We will discuss FIR later in subsequent chapters

From (16) the sequence of coefficients $\{h_k\}_{k \in Z}$ can be represented by its refinement mask [13]. This refinement mask is given as:

$$H(\mathfrak{z}) = \frac{1}{\sqrt{2}} \sum_{k \in Z} h_k \, e^{-2\pi i k \mathfrak{z}} \tag{17}$$

Remark 17: Notice with "z" notation where $z = e^{-2\pi i \mathfrak{z}}$ (17) is a trigonometric polynomial where (16) is the FIR. (17) is then represented as

$$H(z) = \frac{1}{\sqrt{2}} \sum_{k \in Z} h_k \, z^k \tag{18}$$

Theorem 18 ([13], Theorem 7.2) Let $\varphi_{j,k} \in L^2(R)$ be an itegrable scaling function (such as 15). The Fourier series of $\{h_k\}_{k \in Z}$satisfies

$$|H(\mathfrak{z})|^2 + |H(\mathfrak{z} + 1/2)|^2 = 1 \tag{19}$$

(19) is referred to as a *conjugate mirror filter* condition [13]. (19) is a consequence of the orthonormality of the scaling function which is shown in [14], [7]. For more information and proof of Theorem 18 please refer to [13], Theorem 7.2. The main result from Theorem 18 is that (19) is a necessary condition to devise (15). Simply the filters determine several properties of the scaling function.

On the Fourier side of equation (15) we see that

$$\hat{\varphi}(\xi) = H(\xi/2)\hat{\varphi}(\xi/2) \tag{20}$$

It can be shown [14, Meyer] that (20) satisfies (19). An alternative condition for the scaling function is shown below ([13]).

Lemma18.[13],[17]Given a function $f \in L(R)^2$ whose family

$\{f_{0.k} = \tau_k f\}_{k \in Z}$ of integer translates of f is orthonormal if and only if

$$\sum_{n \in Z} \left|\hat{f}(\xi + n)\right|^2 = 1 \tag{21}$$

where $\tau_k f(x) := f(x-k)\ for\ k\ \in Z.$

Proof 19. (inspired by [17]) First we will take the inner product between $\tau_k f$ and $\tau_m f$ with k and m elements of the integers. It follows using a change of variables with the definition of inner product we have

$$\langle \tau_k f, mf \rangle = \langle \tau_{k-m} f, f \rangle$$

For the family of f we may equate their orthonormality via

$$\langle \tau_k f, mf \rangle = \langle \tau_{k-m} f, f \rangle = \langle \tau_K f, f \rangle = \delta_K \ \forall\ m, k, K \in Z$$

Then we will take the Fourier transform on each side of the equation. We know that the Fourier transform will preserve the inner product [ref need]. From the time frequency dictionary the Fourier transform of $\tau_K f$ will translate to a modulation by $e^{-2\pi i k \xi}$ a function whose period is one.

$$\delta_K = \langle \tau_K \hat{f}, \hat{f} \rangle = \int_R e^{-2\pi i k \xi} \left|\hat{f}(\xi)\right|^2 d\xi$$

Then we may use the additive property of the integral to sum the integral over the integers. It follows,

$$\delta_K = \sum_{n \in Z} \int_n^{n+1} e^{-2\pi i k \xi} \left|\hat{f}(\xi)\right|^2 d\xi$$

Next, we will use a change of variables to map the interval [n,n+1) onto a unit interval of [0,1) by setting $m = \xi - n$. Thus the equation above becomes

$$\delta_K = \int_0^1 e^{-2\pi i k \xi} \sum_{n \in Z} \left|\hat{f}(m+n)\right|^2 dm$$

This equation states that the function $F(m) = \sum_{n \in Z} \left|\hat{f}(m+n)\right|^2$ with a period of one as a K^{th}Fourier coefficient equal to the Kroneckerdelta δ_K. It must therefore be equal to one almost everywhere.

■

3.2. **Conjugate Mirror Filters**

Lemma 21. (*Conjugate Mirror Filter***)** Given an orthogonal MRA with a scaling function φ and a corresponding low-pass filter H, where H(ξ) is assumed to be a trigonometric polynomial with period one, the low-pass filter satisfies for almost every ξ.

$$|H(\xi)|^2 + |H(\xi + 1/2)|^2 = 1 \qquad (22)$$

$$H(\xi)\overline{H(\xi)} + H(\xi + 1/2)\overline{H(\xi + 1/2)} = 1$$

Proof 23. [13] Since the scaling function is assumed to be an orthonormal basis and the Fourier transform preserves orthonormality the integer translates of $\hat{\varphi}(\xi)$ will satisfy lemma 34. Thus we have

$$\sum_{n \in Z} |\hat{\varphi}(\xi + n)|^2 = 1 \qquad (23)$$

Plugging equation (20) into (23)we obtain

$$1 = \sum_{n\in Z} |\hat{\varphi}(\xi + n)|^2 = \sum_{n\in Z} \left|H\left(\frac{\xi + n}{2}\right)\right|^2 \hat{\varphi}\left|\left(\frac{\xi + n}{2}\right)\right|^2 \tag{24}$$

Then we will separate the sum over the odd and even integers. It follows,

$$\begin{aligned}\sum_{n\in Z} \left|H\left(\frac{\xi + n}{2}\right)\right|^2 \hat{\varphi}\left|\left(\frac{\xi + n}{2}\right)\right|^2 \\ &= \sum_{n\in Z} \left|H\left(\frac{\xi + 2n}{2}\right)\right|^2 \hat{\varphi}\left|\left(\frac{\xi + 2n}{2}\right)\right|^2 \\ &+ \sum_{n\in Z} \left|H\left(\frac{\xi + 2n + 1}{2}\right)\right|^2 \hat{\varphi}\left|\left(\frac{\xi + 2n + 1}{2}\right)\right|^2 = 1\end{aligned}$$

Next we will use the fact that the function H(z) has period one and factor it out of the integral and obtain

$$\left|H\left(\frac{\xi}{2}\right)\right|^2 \sum_{n\in Z} \hat{\varphi}\left|\left(\frac{\xi}{2} + n\right)\right|^2 + \left|H\left(\frac{\xi}{2} + \frac{1}{2}\right)\right|^2 \sum_{n\in Z} \hat{\varphi}\left|\left(\frac{\xi}{2} + n + \frac{1}{2}\right)\right|^2 = 1$$

Then we can once again use equation (4.5.1) since it is true almost everywhere by substitution we will arrive at

$$\left|H\left(\frac{\xi}{2}\right)\right|^2 + \left|H\left(\frac{\xi}{2} + \frac{1}{2}\right)\right|^2 = 1$$

Finally we may conclude that the equality of the above equation holds everywhere since *H(z)* is a trigonometric polynomial by (18) and is therefore continuous. Hence,

$$H(\xi)\overline{H(\xi)} + H(\xi + 1/2)\overline{H(\xi + 1/2)} = 1$$

■

3.3. The Wavelet and Conjugate Mirror Filters

We saw in (12) the projection of f onto the orthogonal space $\boldsymbol{W_j}$ was given by

$$Q_j f(t) = \sum_{k \in Z} \langle f, \psi_{j,k} \rangle \psi_{j,k}(t)$$

where we denoted $\psi_{j,k}$ by (8).

Theorem 24 ([13], Theorem 7.3) $\psi \in W_0 \subset V_{-1}$ we may express ψ as a superposition of $\varphi_{-1,k}$ where $\varphi_{-1,k}(t)$ forms an orthonormal basis of V_{-1} Meaning, there exists a sequence of coefficients $\{g_k\}_{k \in Z}$ that satisfy the following scaling equation.

$$\psi(t) = \sqrt{2} \sum_{k \in Z} g_k \, \varphi(2t - k) \tag{25}$$

with the unique sequence of coefficients $\{g_k\}_{k \in Z}$ known as the *high-pass filter*.

Theorem 24 [Meyer, 13] Let φ be a scaling function and h the corresponding conjugate mirror filter. The function (25) defined on the Fourier side as

$$\hat{\Psi}(\mathfrak{z}) = G(\mathfrak{z}/2)\hat{\varphi}(\mathfrak{z}/2) \tag{26}$$

with G($\mathfrak{z}$) a trigonometric polynomial whose period is one given by its refinement mask

$$G(\mathfrak{z}) == \frac{1}{\sqrt{2}} \sum_{k \in Z} g_k \, e^{-2\pi i k \mathfrak{z}} \tag{27}$$

where g_k is the *high-pass filter* defined by taking the inverse Fourier transform of (26)

$$g_k = (-1)^{1-k} h(1-k) \tag{28}$$

Lemma 25 ([13], lemma 7.1) The family $\{\psi_{j,k}\}_{k\in Z}$ is an orthonormal basis of $\boldsymbol{W_j}$. if and only if

$$|G(ʒ)|^2 + |G(ʒ + 1/2)|^2 = 1 \tag{29}$$

Proof 26 ([13], lemma 7.1) this proof follows much like **proof** 23. Plugging equation (26) into (21) we obtain

$$1 = \sum_{n\in Z} |\widehat{\psi}(ʒ + n)|^2 = \sum_{n\in Z} \left|\mathrm{G}\left(\frac{ʒ+n}{2}\right)\right|^2 \hat{\varphi}\left|\left(\frac{ʒ+n}{2}\right)\right|^2 \tag{30}$$

Then we will separate the sum over the odd and even integers. It follows,

$$\sum_{n\in Z} \left|G\left(\frac{ʒ+n}{2}\right)\right|^2 \hat{\varphi}\left|\left(\frac{ʒ+n}{2}\right)\right|^2 = \sum_{n\in Z} \left|\mathrm{G}\left(\frac{ʒ+2n}{2}\right)\right|^2 \hat{\varphi}\left|\left(\frac{ʒ+2n}{2}\right)\right|^2 + \sum_{n\in Z} \left|G\left(\frac{ʒ+2n+1}{2}\right)\right|^2 \hat{\varphi}\left|\left(\frac{ʒ+2n+1}{2}\right)\right|^2 = 1$$

Next we will use the fact that the function G(ʒ) has period one and factor it out of the integral and obtain

$$\left|\mathrm{G}\left(\frac{ʒ}{2}\right)\right|^2 \sum_{n\in Z} \hat{\varphi}\left|\left(\frac{ʒ}{2} + n\right)\right|^2 + \left|\mathrm{G}\left(\frac{ʒ}{2} + \frac{1}{2}\right)\right|^2 \sum_{n\in Z} \hat{\varphi}\left|\left(\frac{ʒ}{2} + n + \frac{1}{2}\right)\right|^2 = 1$$

Then we can once again use equation (4.5.1) by substitution we will arrive at

$$\left|G\left(\frac{ʒ}{2}\right)\right|^2 + \left|G\left(\frac{ʒ}{2}+\frac{1}{2}\right)\right|^2 = 1$$

Which is true everywhere since G(ʒ) is a trigonometric polynomial \

■

From the proof above we may conclude that $G(ʒ)$ also satisfies a *conjugate mirror filter* condition and due to the orthogonality between W_0 and V_0 and our definition for $G(ʒ)$ in (27) and (18) we have

$$|H(ʒ)|\overline{|G(ʒ)|} + |H(ʒ+1/2)|\overline{|G(ʒ+1/2)|} = 0 \qquad (31)$$

Chapter 4 Biorthogonality and its Implication

In the previous chapters we introduced an orthogonal MRA and the associated scaling equations. We saw from Mallat's theorem that given an MRA with a scaling function we were guaranteed a wavelet that formed a basis for the orthogonal complement. As a consequence of the orthonormality of the scaling function we discovered conditions on the filter coefficients that insured reconstruction.

The use of FIRs made wavelets very attractive. As the application of wavelets progressed so too did the theory. Practitioners continued to seek wavelets with different properties to solve new problems. These quests for different wavelets with unique properties began with the relaxing of the old. For instance in the following chapter we will discuss an alternative design to an MRA by removing the requirement of orthogonality between a scaling function and its wavelet and discuses the new biorthogonal conditions that insure perfect reconstruction.

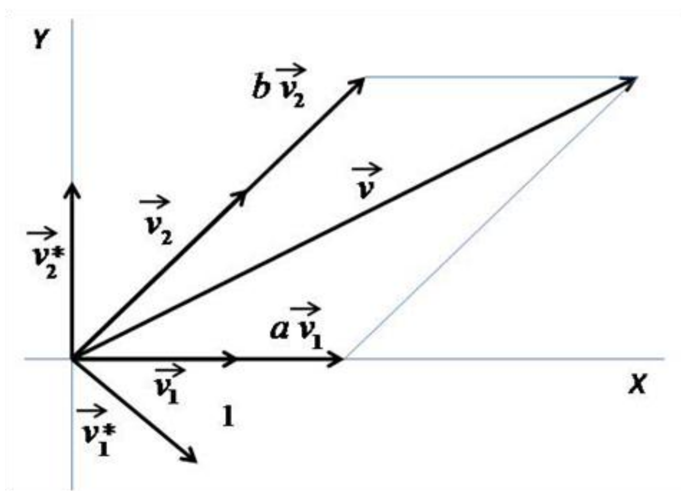

Figure 2. Biorthogonoal Vectors in $\boldsymbol{R^2}$

4.1. Biorthogonal MRA

Example 35 (Simple Biorthogonal Case) Consider the vector s $\overrightarrow{v_1} = (1,0)$ and$\overrightarrow{v_2} = (1,1)$ (Figure 2). We see that they are linearly independent but not orthogonal. These vectors will then form a basis in R^2 such that $\forall\, \vec{v} = (x, y) \in R^2$ There exists unique coefficients a, b such that

$$\vec{v} = a\overrightarrow{v_1} + b\overrightarrow{v_2}$$

In a biorthogonal case, there exist *dual vectors* $\overrightarrow{v_1{}^*}$ and$\overrightarrow{v_2{}^*}$ such that we are able to use the inner products with these *dual vectors* to produce the coefficients a and b where the *dual vectors* satisfy (in our case) $\overrightarrow{v_1{}^*} \perp \overrightarrow{v_2}$ and $\overrightarrow{v_2{}^*} \perp \overrightarrow{v_1}$.

□

Our simple example above leads us to the definition of a biorthogonal basis.

Definitionv36 ([7], Biorthogonal basis) For a Riesz basis $\{\psi_j\}_{j=1}^{\infty}$the dual Riesz basis is a set ofelements$\{\psi^*{}_k\}_{k=1}^{\infty}$ in a space **H** such that$\langle \psi_j, \psi^*{}_k \rangle = \delta_{j,k}$and any $f \in \boldsymbol{H}$ may be expressed as

$$f = \sum_{n=1}^{\infty} \langle f, \psi^*{}_n \rangle\, \psi_n = \sum_{n=1}^{\infty} \langle f, \psi_n \rangle\, \psi^*{}_n$$

A pair of dual Riesz bases ($\{\psi_j\}_{j=1}^{\infty}, \{\psi^*{}_k\}_{k=1}^{\infty}$) of *W will be referred to as a biorthogonal basis.* For the definition of a Reisz bases please refer to the appendix.

Similar to our definition of an orthogonal MRA we also have properties that define a biorthogonal MRA. They are similar in that the scaling function defines the MRA. However we now have two scaling functions and no longer require orthogonality between a scaling function and its associated wavelet.

Definition 37 A **Biorthogonal Multiresolution Analysis** with scaling function φ and dual scaling function φ^*, a biorthogonal MRA satisfies the following properties

$$\forall\, j \in Z,\; V_{j+1} \subset V_j \text{ and } {V^*}_{j+1} \subset {V^*}_j \tag{32}$$

$$\forall\, j \in Z\,, f(t) \in V_j \Leftrightarrow f\left(\frac{t}{2}\right) \in V_{j+1}\; and \tag{33}$$

$$f^*(t) \in {V^*}_j \Leftrightarrow f^*\left(\frac{t}{2}\right) \in {V^*}_{j+1}$$

$$\lim_{j \to +\infty} V_j = \bigcap_{j=-\infty}^{+\infty} V_j = \{0\}\; and \tag{34}$$

$$\lim_{j \to +\infty} V_j^* = \bigcap_{j=-\infty}^{+\infty} {V^*}_j = \{0\}$$

$$\lim_{j \to -\infty} V_j = closure\left(\bigcup_{j=-\infty}^{j=+\infty} V_j\right) = L^2(R) \text{ and} \tag{35}$$

$$\lim_{j \to -\infty} \mathrm{V}_\mathrm{j}^* = closure\left(\bigcup_{j=-\infty}^{j=+\infty} \mathrm{V}_\mathrm{j}^*\right) = L^2(R)$$

The integer translates of φ and φ^* forma a Riesz basis of V_j and V_j^* respectively. (36)

A biorthogonal MRA is very much like an orthogonal MRA in definition, the loss of orthogonality being the key difference. Simply, a biorthogonal MRA consists of two dual MRAs with two scaling functions φ and φ^*. The decomposition of the space $\boldsymbol{L^2}(R)$ given by these two scaling functions is then

$$\ldots V_3 \subset V_2 \subset V_1 \subset V_0 \subset V_{-1} \subset V_{-2} \subset V_{-3} \ldots$$

And

$$\ldots {V_3}^* \subset {V_2}^* \subset {V_1}^* \subset {V_0}^* \subset {V_{-1}}^* \subset {V_{-2}}^* \subset {V_{-3}}^* \ldots$$

Where by (34) the intersection of the spaces is the trivial space $\{0\}$ and by property (35) the union of the spaces is dense.

From property (36) the scaling function $\{\varphi_{j,k}\}_{k\in Z}$ is a Riesz basis for V_j and $\{\varphi^*_{j,k}\}_{k\in Z}$ is a Riesz basis for $V^*{}_j$ ([13], [7]). We also require that these scaling functions be dual in the sense that

$$\langle \varphi_n, \varphi_j^* \rangle = \delta_{n,j}$$

Then for $f \in V_0$,

$$f(t) = \sum_{k\in Z} \langle f, \varphi^*{}_{0,k} \rangle \, \varphi_{0,k}(t)$$

and if $f^* \in {V_0}^*$,

$$f^*(t) = \sum_{k\in Z} \langle f^*, \varphi_{0,k} \rangle \varphi^*{}_{0,k}(t)$$

And just like an orthogonal MRA we can use the scaling functions to traverse across scales. This is seen in property (32 and 33).

Unlike an orthogonal MRA, the spaces V_j and W_j are no longer orthogonal (also true for the spaces V_j^* and W_j^*). We still relate the spaces by

$$V_j = V_{j+1} \oplus W_{j+1}$$

and

$$V_j^* = V_{j+1}^* \oplus W_{j+1}^*$$

Only this time we impose the following conditions

$$V_j \perp W_j^* \text{and } V_j^* \perp W_j$$

Where $\{\psi_{j,k}\}_{k \in Z}$ and $\{\psi^*{}_{j,k}\}_{k \in Z}$ are dual bases for W_j and W_j^*, respectively.

4.2. Biorthogonal Scaling equations

For a biorthogonal MRA the basic scaling equations (from [13]) are

$$\varphi(t) = \sqrt{2} \sum_{k \in Z} h_k \, \varphi(2t - k) \; and \; \varphi^*(t) = \sqrt{2} \sum_{k \in Z} h_k^* \, \varphi^*(2t - k) \tag{37}$$

$$\psi(t) = \sqrt{2} \sum_{k \in Z} g_k \, \varphi(2t - k) \; and \; \psi^*(t) = \sqrt{2} \sum_{k \in Z} g_k^* \, \varphi^*(2t - k) \tag{38}$$

And on the Fourier side of these equations become

$$\hat{\varphi}(\mathfrak{z}) = H(\mathfrak{z}/2)\hat{\varphi}(\mathfrak{z}/2) \text{ and } \hat{\varphi}^*(\mathfrak{z}) = H^*(\mathfrak{z}/2)\hat{\varphi}^*(\mathfrak{z}/2) \tag{39}$$

$$\hat{\psi}(\mathfrak{z}) = G(\mathfrak{z}/2)\hat{\varphi}(\mathfrak{z}/2) \text{ and } \hat{\psi}^*(\mathfrak{z}) = G^*(\mathfrak{z}/2)\hat{\varphi}^*(\mathfrak{z}/2) \tag{40}$$

Similar to what we observed in the orthogonal case, the scaling equations (insert here) in the biorthogonal MRA are defined implicitly from the dual scaling functions.

4.3. **Finite Impulse Response Filters and Fast Wavelet Transform**

From (39) we can define the set of four FIR. With their refinement mask and using "z" notation we have

$$H(z) = \frac{1}{\sqrt{2}}\sum_{k\in Z} h_k\, z^k \text{ and } H^*(z) = \frac{1}{\sqrt{2}}\sum_{k\in Z} h_k^*\, z^k \tag{41}$$

with

$$G(z) = z\overline{H^*(z)} \text{ and } G^*(z) = z\overline{H(-z)} \tag{42}$$

And due to the biorthogonality we will have the following conditions

$$H(z)\overline{H^*(z)} + H(-Z)\overline{H^*(-Z)} = 1$$

$$G(z)\overline{G^*(z)} + G(-Z)\overline{G^*(-Z)} = 1$$

$$H(z)\overline{G^*(z)} + H(-Z)\overline{G^*(-Z)} = 0$$

$$G(z)\overline{H^*(z)} + G(-Z)\overline{H^*(-Z)} = 0$$

4.4. **Fast Wavelet Transform**

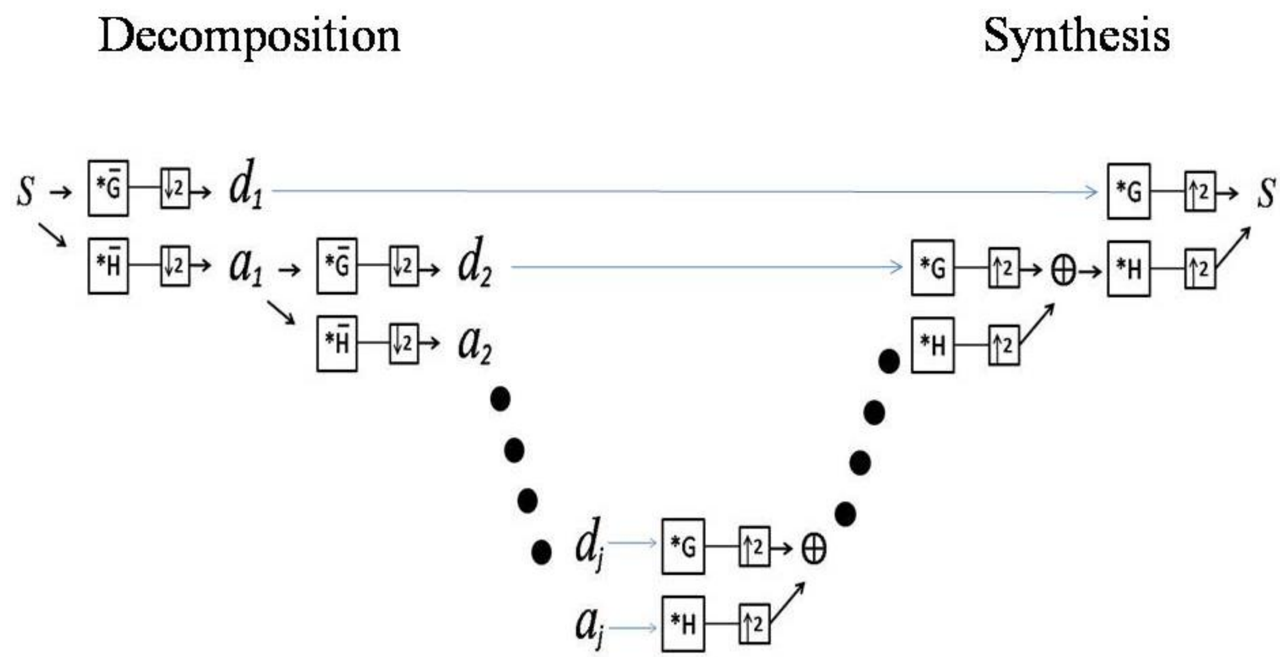

Figure 3

Biorthogonal Fast Wavelet Transform Schematic

Using the biorthogonal FIR (41,42) we may implement a fast wavelet transform for a signal S (Figure 3). On the side of decomposition the * symbol is used to denote a convolution with the conjugate flip (denoted by a line over the filter) of the *high-pass filter* G^* and *low-pass filter* H^* and the $\downarrow 2$ is the down sampling operator were every even sample is removed. With the reconstruction or Synthesis, the approximation and detail is convolved with the filters *G* and *H*. The $\uparrow 2$ is the up sampling operator adding in zeros in the even indexes of the approximation or detail. The $\oplus$ is the orthogonal summation.

Chapter 5 Wavelets and Electroencephalography

5.1. Materials and Methods

Data Collection

EEG from 116 participants was collected as part of a study conducted at the Hartford Hospital. The participants were either a healthy control group (HC group, N = 58) or a group of participants diagnosed with schizophrenic spectrum psychological disorders (SZ group, N = 58). The standard 10-20 electrode placement was used with 64 Electrodes. The HC and SZ groups participated in a standard auditory oddball paradigm where they pressed a button when a target tone (1000 Hz) appeared within a series of standard auditory tones (1500 Hz). A total of 656 tones (20% targets) were presented to participants during the experiment.

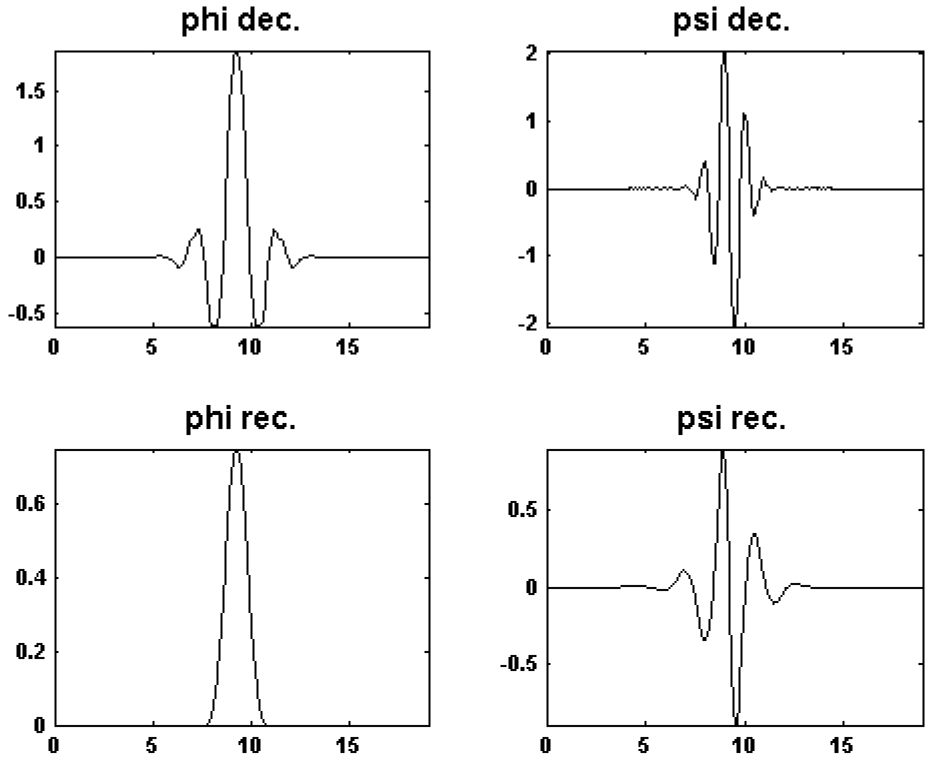

Figure 4.Dual Scaling and Dual Wavelet Functions for the Biorthogonal Spline.

Finite Impulse Response Filters for the Biorthogonal Spline Wavelet Transform			
Low Decomposition	**High Decomposition**	**Low Reconstruction**	**High Reconstruction**
-0.0007	0	0	-0.0007
0.0020	0	0	-0.0020
0.0051	0	0	0.0051
-0.0206	0	0	0.0206
-0.0141	0	0	-0.0141
0.0991	0	0	-0.0991
0.0123	0	0	0.0123
-0.3202	0	0	0.3202
0.0021	-0.1768	0.1768	0.0021
0.9421	0.5303	0.5303	-0.9421
0.9421	-0.5303	0.5303	0.9421
0.0021	0.1768	0.1768	-0.0021
-0.3202	0	0	-0.3202
0.0123	0	0	-0.0123
0.0991	0	0	0.0991
-0.0141	0	0	0.0141
-0.0206	0	0	-0.0206
0.0051	0	0	-0.0051
0.0020	0	0	0.0020
-0.0007	0	0	0.0007

De-noising and filtering

Independent component analysis was used to remove artifacts from the raw EEG. The bi-orthogonal spline wavelet (represented by the finite, bi-orthogonal, filter banks, see table above) was convolved with individual time series to calculate wavelet coefficients and to decompose the EEG into time-frequency representation. These time-frequency representation approximate the Hi-Gamma (65 – 125 Hz), gamma (32 – 65 Hz), Beta (16 – 32 Hz), alpha (8 – 16 Hz), theta (4 – 8 Hz), and delta (0-4 Hz) frequency bands. Analysis was focused on the delta and theta frequency bands since they have the strongest contribution to the EEG response to targets [23]

Comparative wavelet analysis

Individual trials were decomposed using the fast biorthogonal wavelet transform and the wavelet coefficients were averaged separately for the 5 octaves and residual space for target and non-target EEG segments. This was done for channels Fz, Cz, and Pz. A two-way-ANOVA was conducted separately for each octave and residual space, and channel, in order to identify coefficients which demonstrate a significant interaction between group (HC and SZ) and stimulus type (target or non-target). The coefficient and EEG electrode with the smallest p-value was used as a feature in the subsequent analysis.

5.2. **Results, Conclusions and Closing Remarks**

For the channels PZ, CZ, and FZ, a two-way ANOVA was conducted with the following results:

Using the wavelet transform, the coefficients for responses were calculated for the HC and SZ groups. The 14th coefficient, which lies in the delta residual band statistically differentiated responses between target tones and non-target tones (Targetness), and differentiated individuals within the groups.

Analysis of Variance **Channel PZ**					
Source	**Sum Sq.**	**d.f.**	**Mean Sq.**	**F**	**Prob>F**
Subject	1786.4	1	1786.4	21.91	0
Targetness	12481.6	1	12481.6	153.1	0
Subject * Targetness	1119	1	1119	13.73	.0003
Error	18587.9	228	81.5		
Total	33974.9	231			

Analysis of Variance Channel CZ					
Source	**Sum Sq.**	**d.f.**	**Mean Sq.**	**F**	**Prob>F**
Subject	83.3	1	83.35	.079	.0376
Targetness	14968	1	14968.04	141.31	0
Subject * Targetness	243.2	2	243.22	2.3	0.1311
Error	24150	228	105.92		
Total	39444.6	231			

Analysis of Variance Channel FZ					
Source	**Sum Sq.**	**d.f.**	**Mean Sq.**	**F**	**Prob>F**
Subject	53.5	1	53.5	.034	.05585
Targetness	4545.7	1	4545.74	29.17	0
Subject * Targetness	0	1	0.01	0	0
Error	35526.9	228	155.82		
Total	40126.1	231			

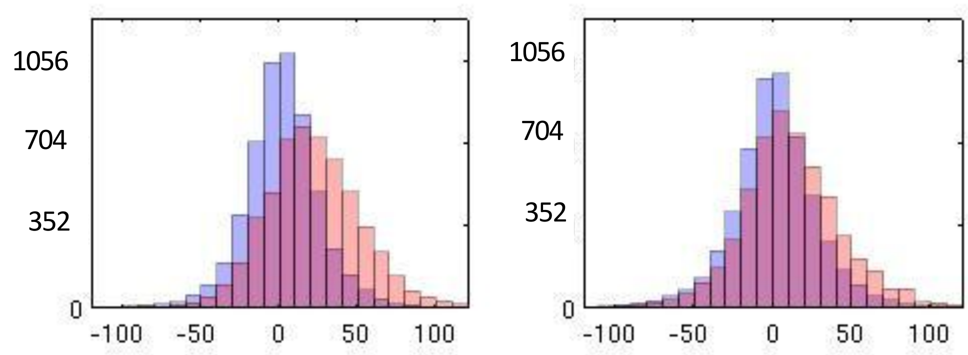

Figure 5. The histogram for the 14th coefficient for HC group, left and SZ group, right.

Figure 5, above, for the HC (left) have 76% of their delta coefficients for target responses above zero, while the SC group has 64% (orange data series). Both groups HC and SZ had approximately a 50/50 distribution for the non target responses for the delta 14 coefficient below zero and above zero (blue series).

These results demonstrate the time-frequency characteristics in which ERP responses are sensitive to acoustic regularities in healthy controls and individuals with schizophrenia.

Appendix

Definition A1 (Inner Product) Astrictly positive-definite) inner product on a vector space V over C (the complex numbers) is a function $\langle .,. \rangle : VxV \rightarrow C$ such that for , all x, y, z $\in$ V and α, β $\in$ C,

(i) $\langle x, y \rangle = \overline{\langle y, x \rangle}$

(ii) $\langle \alpha x + \beta y, z \rangle = \alpha \langle x, z \rangle + \beta \langle y, z \rangle$

(iii) $\langle x, x \rangle \geq 0$

(iiii) $\langle x, x \rangle = 0 \; iff \; x = 0$

Bibliography

[1.] Adelia, Hojjat, Zhou, Ziqin, and Dadmehr, Nahid. “Analysis of EEG records in an epileptic patient using wavelet transform.” Journal of Neuroscience Methods 123 (2003): 69-87. Print.

[2.] Ademoglu,Ahmet, Micheli-Tzanakou,Evangelia, and Istefanopulos,Yorgo. “Analysis of Pattern Reversal Visual Evoked Potentials (PRVEP’s) by Spline Wavelets.” EEE Transactions on Biomedical Engineering, Vol. 44, No. 9, (1997): 881–890. Print.

[3.] Barford, Lee A., R. Fazzio, Shane, and Smith, David R. Instruments and Photonics Laboratory. “An Introduction to Wavelets.” HPL-92-124, (September, 1992): 1–27.

[4.] BasarErol, Demiralp Tamer, Schürmann Martin, Basar-ErogluCanan, and AdemogluAhmet. “Oscillatory Brain Dynamics, Wavelet Analysis, and Cognition.” Brain and Language 66, (1999): 146–183. Print.

[5.] BasarErol, Schürmann, Martin, Demiralp, Tamer, Basar-Eroglu, Canan, and Ademoglu, Ahmet. “Event-related oscillations are ‘real brain responses’ — wavelet analysis and new strategies.” International Journal of Psychophysiology 39 (2001): 91–127. Print.

[6.] Beck, Travis W., Housh, Terry J., Johnson Glen O., Weir, Joseph P., Cramer, Joel T., Coburn, Jared W., and Malek, Moh H. “Comparison of Fourier and wavelet transform procedures for examining the mechanomyographic and electromyographic frequency domain responses during fatiguing isokinetic muscle actions of the biceps brachii.” Journal of Electromyography and Kinesiology 15 (2005): 190–199. Print

[7.] Daubechies, Ingrid. Ten Lectures on Wavelets. Montpelier, VT: Capital City Press (1994). Print.

[8.] Demiralp, Tamer, Ademoglu, Ahmet, Schürmann, Martin, Basar-Eroglu, Canan, and Basar, Erol. “Detection of P300 Waves in Single Trials by the Wavelet Transform (WT).” Brain and Language 66, (1999): 108–128. Print.

[9.] Demiralp, Tamer, Yordanova, Juliana, Kolev, Vasil, Ademoglu, Ahmet, Devrim, Müge, and Samar, Vincent J. "Time–Frequency Analysis of Single-Sweep Event-Related Potentials by Means of Fast Wavelet Transform." Brain and Language 66, (1999): 129–145. Print.

[10.] Demiralpa, Tamer, Ademoglub, Ahmet, Istefanopulosb, Yorgo, Basar-Erogluc, Canan, and BasarErol. "Wavelet analysis of oddball P300." International Journal of Psychophysiology 39 (2001): 221–227. Print.

[11.] Hostens, I., Seghers, J., Spaepen, A., and Ramon, H. "Validation of the wavelet spectral estimation technique in Biceps Brachii and Brachioradialis fatigue assessment during prolonged low-level static and dynamic contractions." Journal of Electromyography and Kinesiology 14 (2004): 205–215. Print.

[12.] Kamont, Anna and Passenbrunner, Markus. "UNCONDITIONALITY OF ORTHOGONAL SPLIN SYSTEMS IN H1." Cornell University arXiv:1404.5493 [math.FA], (2014). Print.

[13.] Mallat,Stáphane, with contributions from Peyré, Gabriel. A WAVELET TOUR OF SIGNAL PROCESSING.Third edition. Burlington, MA: Academic Press (1999). Print.

[14.] Mallat,Stephane, G., "MULTIRESOLUTION APPROXIMATIONS AND WAVELET ORTHONORMAL BASES OF L2(R)." Transactions of the American Mathematical Society. Volume 315, Number 1 (1989): 69–87. Print.

[15.] Misiti, Michel, Misiti, Yves, Oppenheim, Georges, and Poggi, Jean-Michel. Wavelet Toolbox for Use with MATLAB®. Natick, MA: The MathWorks, Inc. (1996). Print.

[16.] Mohlenkamp, Martin J. and Pereyra, María Christina. Wavelets, Their Friends, and What They Can Do for You. Edinburgh, U.K.: European Mathematical Society (2008). Print.

[17.] Pereyra, María Christina, and Lesley A. Ward. Harmonic Analysis: From Fourier to Wavelets. Providence, RI: American Mathematical Society, 2012. Print.

[18.] Quiroga,Quian R. and Garcia, H. “Single-trial event-related potentials with wavelet denoising.” Clinical Neurophysiology 114 (2003): 376–390. Print.

[19.] Quiroga, Quian R., Sakowitz, O.W., Basar, E., and Schürmann,M. “Wavelet Transform in the analysis of the frequency composition of evoked potentials.” Brain Research Protocols 8 (2001): 16–24. Print.

[20.] Rosso, O.A., Martin, M.T., Figliola, A., Keller, K., and Plastino, A. “EEG analysis using wavelet-based information tools.” Journal of Neuroscience Methods 153 (2006): 163–182. Print.

[21.] Samar, Vincent J. “Wavelet Analysis of Neuroelectric Waveforms.” Brain and Language 66, (1999): 1–6. Print.

[22.] Samar, Vincent J. “Wavelet Analysis of Neuroelectric Waveforms: A Conceptual Tutorial.” Brain and Language 66, 7–60 (1999). Print.

[23.] Demiralp, T. (1999) 'Detection of P300 waves in single trials by the wavelet transform (WT)', Brain and Language, vol. 66, pp. 108-128.

[24.] Jeon, Y.W. (2003), 'Meta-analysis of P300 and schizophrenia: patients, paradigms, and practical implications', Psychophysiology, vol. 40, pp. 684-701.